Proceedings of the 2011 International Mechanical Engineering Congress and Exposition
ASME/IMECE2011
November 11-17, 2011, Denver, Colorado, USA

IMECE 2011-64333

UNSTEADY FLOW CHARACTERISTICS AND VISCOUS FLOW LOSSES BEHIND MULTIPLE ROWS OF CIRCULAR PIN FINS IN COOLANT CHANNELS

Zeki Ozgur Gokce[1]
Turbomachinery Aero-Heat Transfer Laboratory
Department of Aerospace Engineering
The Pennsylvania State University
University Park, Pennsylvania 16802
Email: zog100@psu.edu

Cengiz Camci[2]
Turbomachinery Aero-Heat Transfer Laboratory
Department of Aerospace Engineering
The Pennsylvania State University
University Park, Pennsylvania 16802
Email: cxc11@psu.edu

ABSTRACT

This article deals with a computational assessment of 3D viscous flow behind multiple rows of circular pin fins in coolant channels used in gas turbine systems. Unsteady oscillations and turbulent flow characteristics especially near the endwall surfaces generate the much needed heat transfer enhancement that is usually from the walls to the coolant fluid. The current study is about a comprehensive assessment of present day computational fluid dynamics solvers for the enhancement of wall to coolant heat transfer rates. The paper presents details regarding many flow characteristics, including particle streamlines, as well as total pressure, turbulent kinetic energy and hub heat transfer coefficient contours. The endwall fence placed upstream of the cylinder generates a measurable increase in heat transfer rates downstream of the cylinder. The paper also includes a number of suggested ways to enhance endwall heat transfer rates for use in gas turbine cooling configurations and total pressure improvements near the turbine hub endwall.

INTRODUCTION

The flow around the Nozzle Guide Vanes (NGVs) and the circular pin fins are of special interest to gas turbine studies: The behavior of the former affects the total pressure level downstream of the NGV, hence the efficiency of the gas turbine. The behavior of the latter affects the properties of the coolant which flows within the cooling channels of the NGVs and turbine rotor blades. Therefore, the necessity of understanding and if possible, improving the characteristics of the flow phenomena in mention would be an important development in gas turbine technology.

One of the most crucial components of modern jet engines is the gas turbine. Horseshoe vortices which form around turbine NGVs and rotor blades create a viscous loss which has a detrimental effect on the gas turbine's efficiency [1]. Compared to the freestream flow, the endwall boundary layer contains a momentum deficit, which is the main reason behind the generation of the horseshoe vortex [2]. A portion of the hot gas mixture of air and fuel is transported by the horseshoe vortices from the combustor exit towards the NGVs. Turbine cooling characteristics could be improved if the location at which such vortices form, the path they follow and their aerodynamic behavior were known. As a result, the allowed operational total temperature at the turbine inlet would be larger, which would also imply the presence of a higher turbine efficiency [3], [4]. In addition, the convection of horseshoe vortices into turbine passages which contain high speed flows create a noticeable total pressure loss. All of these factors urge the necessity to understand and improve the conditions imposed by the horseshoe vortex.

The superposition of two physical features creates a roll-up within the streamwise plane of symmetry: First, at a wall saddle point, the presence of the wall boundary layer leads to the separation of the fluid from the hub endwall [5]. Since the freestream flow has larger momentum compared to the boundary layer flow, the flow which stagnates near the saddle point undergoes a rolling motion [5]. Second, the bluff body located downstream imposes an adverse pressure gradient, which is impossible for the fluid to compensate for after a certain point [6]. Subsequently, the roll-up in mention progresses downstream in the shape of a horseshoe.

In the past, a number of experimental work has been conducted to investigate the behavior of horseshoe vortices and the effects accompanying them [5-11]. Praisner and Smith studied the time dependent characteristics of and the heat transfer in the vicinity of a horseshoe vortex around a body having a symmetric airfoil profile [8], [9]. Hada et al. observed that the heat transfer near the leading edge-hub endwall junction was strongly influenced by the leading edge diameter in their study which contains a computational validation of their experiments

[1] Graduate Research Assistant, Ph.D Candidate
[2] Professor of Aerospace Engineering

[10]. An important number of experiments and the resulting data has been provided in the studies of Eckerle [6] and Eckerle and Langston [5], which contain the analysis of horseshoe vortex formation around a vertical cylinder in cross flow. A correlation based on the Reynolds number calculated using the diameter of the cylinder has been provided in Eckerle and Awad [7]. Utilizing endwall fences placed within turbine passages and the turbine environment in general has been shown to be beneficial by a number of researchers [12-14]. The literature on horseshoe vortices and turbine aerodynamics in general suggests that modifying the endwall shape at aerodynamically crucial locations could result in fewer losses.

Turbine blades can be cooled in a more efficient manner by increasing the heat transfer within their cooling channels without inducing a high total pressure loss. Various alignments of cylindrical pin fins serve very well for this purpose, because the presence of the pin fin creates a flow of increased turbulence and unsteady character, compared to the simple arrangement of the channel not containing pin fins.

An important number of cooling pin fin studies have been conducted with various geometries, circular and non-circular alike. VanFossen's work [15] is an experimental study which investigates the effect of placing rows of straight or inclined pin fins to ascertain their effect on heat transfer levels. A comparison of long versus short pin fins (shorter than 4 cylinder diameters in length) is also made; the results indicate that the heat transfer coefficients on the pin surface are 35% higher than the endwall surface, and that short pin fins create an important increase in heat transfer levels when compared to the channel with no fins installed. Metzger and Haley [16] realized an experimental study where rows of short pin fins made out of heat conducting and non-heat conducting material were used to analyze the effect they had on heat transfer. It was observed that both the non-conducting and conducting pin fins generated a similar result, and both showed an increase in heat transfer when compared to the channel with no fins installed. Uzol and Camci [17] have conducted an experimental study consisting of three different pin fin arrays. They have obtained measurements using Liquid Crystal Thermography and Particle Image Velocimetry (PIV) techniques, for pin fin geometries which are circular, simple elliptic (SEF) and N-type (consisting of a NACA 4-digit profile). The circular pin fin array resulted in a 27% increased heat transfer rate compared to the other geometries, whereas the SEF and N-type fin arrays performed better in terms of total pressure loss. Chang et al. [18] realized an experimental study which investigated the effect of placing a circular pin fin with no tip clearance (distance between the fin tip and endwall) and fins with varying amounts of clearance. It was shown that improvements in total pressure loss levels are obtained with moderate heat transfer decreases.

Building an experimental setup to investigate fluid properties around a NGV blade and/or a pin fin is possible; however, it will be an expensive endeavor, both in terms of time and funds. On the other hand, thanks to the high computing capabilities of modern computers, modeling the flow within such domains with the use of Computational Fluid Dynamics (CFD), is a fast and economical method. Furthermore, the best results obtained using CFD will suggest optimum configurations, and a lot of time and resources may be saved by experimenting only with such optimum configurations.

Keeping in mind the points mentioned about the flow around a NGV, and after having studied the previously published work, we conducted 2 CFD based studies [19], [20]. Throughout these studies, we had decided to model the NGV blade as a circular cylinder, where the diameter of the cylinder is proportional to the leading edge diameter of the blade. The leading edge diameter of the NGV is the dominant factor which affects horseshoe vortex formation around the blade and near the hub, and as such, it is reasonable to use this proportionality in the numerical computations. The main idea behind these studies, was to insert an endwall fence upstream of the cylinder, which would in turn partially or totally relieve the adverse effects of the horseshoe vortex from the flow domain, and successfully modify the location of the main roll-up and subsequent horseshoe vortex. This main goal was desired to be achieved without affecting the freestream region. The results indicated that these goals were attained [19], [20].

Considering the important aspects of cooling flow within NGV and rotor blades, the published research on the topic, and following the results obtained in our previous works [19], [20], we decided to analyze the heat transfer and cooling aspects of such flows, along with the heat transfer aspect of flow around a NGV. The circular cylinder is a good representative of the circular pin fins located within the cooling channels of turbine blades as well, therefore the circular cylinder model we use in our CFD calculations is perfectly suitable for investigating cooling flow within cooling channels, along with the flow in the vicinity of a NGV. The heat transfer aspect of the flow was incorporated by solving the energy equation along with the other governing equations. The main idea behind the current study is to place endwall fences upstream of the cylinder leading edge, with the goal of attaining an increase in heat transfer rates and a decrease in the total pressure loss downstream of the cylinder. The simulations were run for a single cylinder, however, the results for the single cylinder can easily be interpreted for a row of multiple cylinders.

The CFD simulations were carried out with the commercially available software FLUENT which is developed by ANSYS. The k-ω model with Shear Stress Transport (SST) has been used due its reputation for generating good results with flows containing adverse pressure gradients. The flow within our domain has a Reynolds number of 11000, which indicates that the cylinder wake will be subject to unsteady vortex shedding. Therefore, the simulations were conducted on a time-dependent basis. In order to validate the modeling strategy we have used, we have compared the results generated by our strategy with previously published experimental data for a conventional cylinder in cross flow [6].

The results indicate that the flow within the cylinder wake exhibits a periodic unsteady vortex shedding. The effects of the horseshoe vortex do not extend into the freestream, and they are

limited within the first 2-3 mm region above the hub endwall. The presence of the endwall generates an increase in turbulent kinetic energy levels within the cylinder wake. Hence, a higher amount of heat transfer - an average of 10% increase when compared to the baseline case with no fence installed - towards the hub surface is observed within the cylinder wake. This is a very important result for circular pin fins, because increased heat transfer coefficient levels over the hub surface implies that improved cooling can be achieved through the application of such fences. The mass averaged total pressure levels within 2 mm high rectangular portions placed right above the hub surface indicate that the presence of an endwall fence results in a decreased amount of mass averaged total pressure loss. This is a critical result for gas turbine applications where any increase in total pressure levels downstream of NGVs and rotor blades is a welcome change. The total pressure contours within horizontal planes placed 2.5 and 3 mm apart of each other are also presented. The plots which contain time-dependent properties are gathered in video files, and are presented in video form.

The conclusions drawn from this study are very important because they demonstrate that the usage of upstream endwall fences successfully generate improvements in the heat transfer properties of circular pin fins in cooling channels, as well as decreases in total pressure losses near the hub downstream of NGV blades. Our research group is continuing to work in this field.

NOMENCLATURE

Re_D = Reynolds number based on the cylinder diameter = $\frac{\rho U_\infty D}{\mu}$

ρ = Density (kg/m^3)

μ = Viscosity (kg/m.s)

$U_\infty = U_{Inlet}$ = Freestream velocity in the streamwise direction (m/s)

$U_{Profile}$ = Inlet velocity profile (m/s)

k = Turbulent kinetic energy (m^2/s^2) = $\frac{3}{2}(U_{Profile} I)^2$

ω = Magnitude of vorticity (1/s) = $\frac{k^{1/2}}{l c_\mu{}^{1/4}}$

I = Turbulence intensity (%)

l = Turbulence length scale (m)

c_μ = A coefficient related to the k- ω SST turbulence model

h = Heat transfer coefficient (W/m^2.K)

x = Streamwise direction

y = Lateral direction

z = Vertical direction

P_S = Static pressure (Pa)

P_0 = Total pressure (Pa)

$C_{P_S} = \frac{P_{S_{Cylinder}} - P_{S_{Inlet}}}{\frac{1}{2}\rho U_{Inlet}{}^2}$ = Static pressure coefficient

$C_P = \frac{(P_0)_{YZ\ plane} - (P_0)_{Inlet}}{\frac{1}{2}\rho (U_{Inlet})^2}$ = Mass averaged total pressure based C_p within complete y-z planes

$C_P = \frac{(P_0)_{2\ mm\ Strip} - (P_0)_{2\ mm\ Inlet\ Strip}}{\frac{1}{2}\rho (U_{2\ mm\ Inlet\ Strip})^2}$ = Mass averaged total pressure based C_p within 2 mm high rectangular y-z planes

D = Cylinder diameter (m)

St = Strouhal number

f = Frequency (Hz)

NUMERICAL METHOD

A commercially available software (FLUENT version 12.1, developed by ANSYS) was used to realize the numerical modeling of the flow around the vertical cylinder and the fence configuration. The meshing of the computational domain was performed with another software (GAMBIT), developed by the same company. The accuracy of results obtained by combining these two software programs was demonstrated by a relevant validation study.

The computational domain consisted of a vertical cylinder of 12 mm diameter and 18 mm height placed in a rectangular field, which has the same height as the cylinder, has a width of 63 mm and length of 336.9 mm. The origin of the coordinate system was placed at the center of the lower circular surface of the cylinder. The mid-span axial chord length of the NGV blade used by Turgut [21], Kavurmacioglu et al. [22,23] and Rao et al. [24] which equaled 112.3 mm, was used as a length scale; the domain covers the area between a point one mid-span axial chord length upstream of the cylinder center, and a point two mid-span axial chord lengths downstream. The width of the domain was 63 mm and 5.25 times the cylinder diameter, and the height of the domain was 18 mm and equal to the cylinder height; in order to accurately capture and model all flow phenomena, these dimensions were chosen since they are sufficiently large to reach this goal. Note that, even though the domain is created based on the dimensions of a NGV blade, it can also very effectively symbolize a circular pin fin. Note that the height-to-diameter ratio of the cylinder is 1.5, which is a

reasonable value for pin fins which are considered as heat transfer promoters [15, 16].

The baseline case consisted of a cylinder only, with no fence installed. For the fence-installed case (the case containing the upstream fence - hereafter referred to as the fence-installed case), a rectangular fence is placed 24 mm upstream of the cylinder center in order to successfully alter the aerodynamic and thermal properties of the flow. This specific location was chosen due to its potential to achieve the goals in mention: The distance between the fence and the cylinder will serve to generate an increased roll-up, which will in turn generate an increase in heat transfer rates downstream of the cylinder, as well as an increase in total pressure levels near the hub endwall.

Figures 1 through 6 demonstrate the main geometrical properties of the baseline and fence-installed cases as seen from various perspectives:

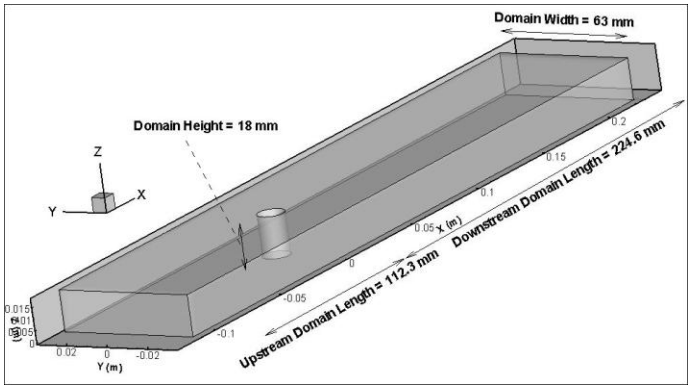

Figure 1. Three dimensional overview of the baseline case

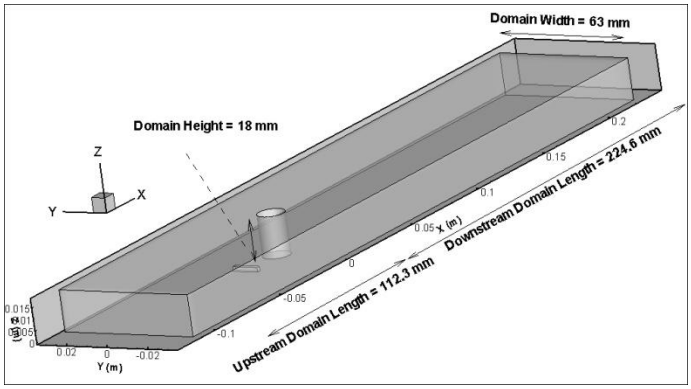

Figure 2. Three dimensional overview of the fence-installed case

The flow within the turbine environment and the cooling channel inside the turbine blades is highly turbulent, therefore it contains high gradients for many fluid parameters. The complexity of such a type of flow requires the use of a structured mesh, which has the quality of effectively capturing flow parameter gradients throughout the domain. Locations of critical aero-thermodynamic influence, including the junction of the cylinder and the hub endwall, the junction of the fence and the hub endwall, as well as the first 3 millimeters above the hub endwall which contain the boundary layer and the horseshoe vortex, were diligently meshed during the generation of the computational domain.

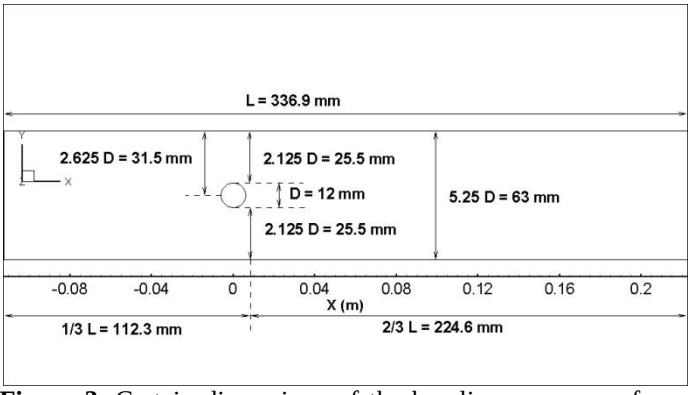

Figure 3. Certain dimensions of the baseline case, seen from the top

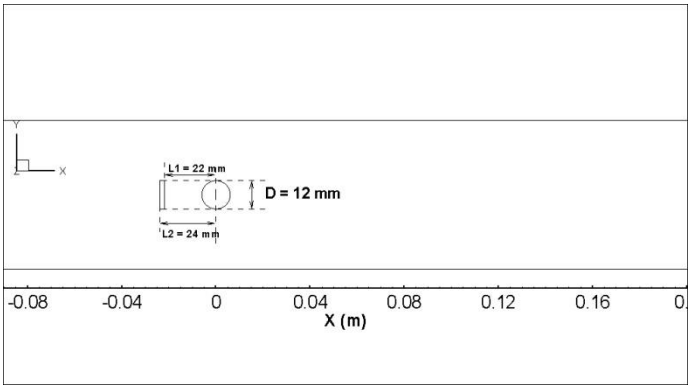

Figure 4. Certain dimensions of the fence-installed case, seen from the top

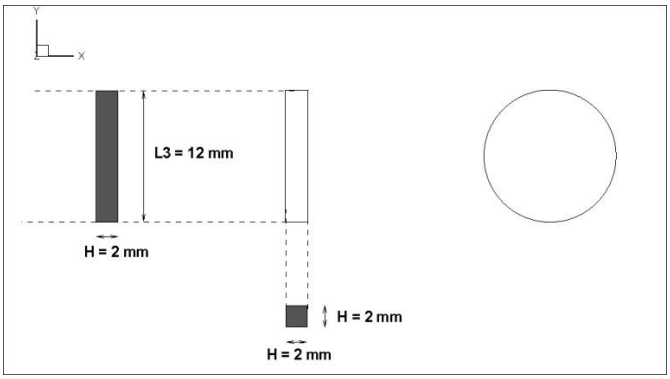

Figure 5. Cross section details of the fence

For both cases, the region surrounding the cylinder and the first few millimeters above the hub endwall are of great aero-thermodynamic significance. In addition, for the fence-installed case, the fence-hub endwall junction is very important. In order to capture even subtle flow events within these regions, their geometrical boundaries were very densely meshed. Due to the uniformity of the flow at locations outside the boundary layer

region and the vicinity of the cylinder, the following adjustments were made to the mesh structure in order to decrease the computational time: As we proceed from the cylinder center towards the inlet and outlet of the domain, the mesh is stretched so that nodes are spaced less closer to each other. In addition, an increase in edge mesh lengths is seen when we proceed from the hub towards the top of the domain.

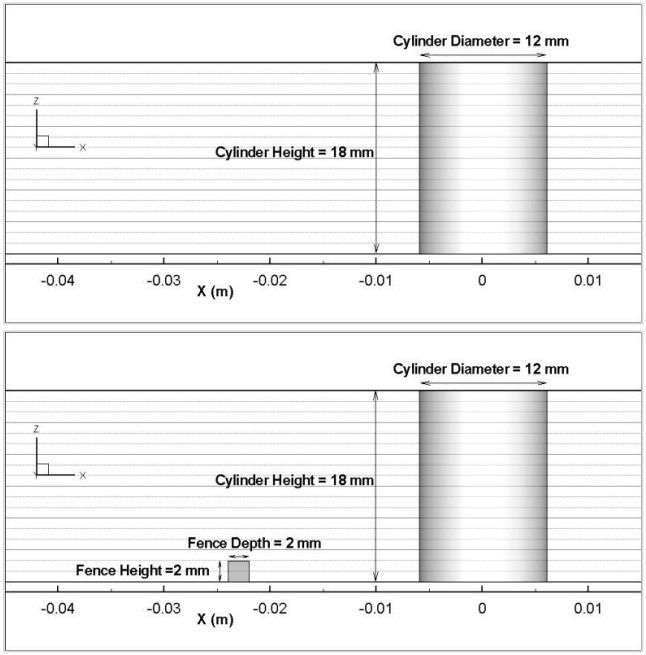

Figure 6. Certain dimensions demonstrated within the x-z plane, for the baseline and fence-installed cases, respectively

A two-equation turbulence model was preferred for our study since such models provide a fine balance between accuracy and fast computing. The k-ω model with Shear Stress Transport (SST) was chosen thanks to the good results it produces when used for a flow containing a high adverse pressure gradient.

Fluent's pressure based, implicit solver was utilized throughout the calculations. The computations were run under unsteady conditions, due to the unsteady nature of the cylinder wake for the Reynolds number we are interested in. The natural time step for the process was 4.3 ms, which was calculated by inverting the frequency obtained using the experimental Strouhal number of 0.2 for a cylinder from the following formula:

$$St = \frac{fD}{V} \qquad (\mathbf{1})$$

where the frequency is found to be equal to 233 Hz by setting the cylinder diameter to 0.012 m and velocity to the freestream value of 14 m/s. The actual time step used was 0.086 ms, because a time step this small (1/50 of the natural time step) will convey the natural unsteadiness of the wake and capture even the smallest variation in flow behavior. 20 pseudo-time steps were used at each time step to keep the residual levels at a small average value. The solution scheme used second order discretizations for all the terms in the solution equations. The pressure-velocity coupling was set to the "coupled" mode. The energy equation was also solved in order to model the heat transfer occurring throughout the domain.

The velocity values obtained by extensive measurements by Zaccaria [25] during his studies were used to form the inlet velocity profile. The Reynolds number of the flow is 11000, which is calculated based on the cylinder diameter. The flow within cooling channels and the flow downstream of the combustor is fully turbulent; therefore the computations were conducted using fully turbulent flow. Incompressible flow was assumed. The gas was assumed to be hotter than the cylinder, hub endwall and the fence: The gas temperature was set to 500 K and the walls to 300 K.

The turbulence kinetic energy, *k*, and the magnitude of vorticity, *ω*, were used as the turbulence criteria. These were calculated according to the following formulas:

$$k = \frac{3}{2}(U_{Profile} I)^2 \qquad (\mathbf{2})$$

$$\omega = \frac{k^{1/2}}{l c_\mu^{1/4}} \qquad (\mathbf{3})$$

where a turbulence intensity (*I*) of 1% and a turbulence length scale (*l*) of 18 mm were used, along with a mean freestream velocity profile [25], and a k-ω with SST turbulence model related coefficient (c_μ) of 0.09. The maximum possible eddy length, which was the cylinder height of 18 mm was considered as the turbulence length scale. Standard values were selected for the inlet static pressure, air density and viscosity.

Two validation studies were conducted in order to make sure that the modeling strategy used during the computational process - the meshing conducted in Gambit and subsequent simulations carried out by using Fluent - is accurate. The first of such studies was to numerically re-generate the results of a previously published experimental work involving a vertical cylinder in cross flow mounted on a wall: Eckerle's Ph.D thesis [6] was chosen to be used for this step.

A large quantity of data, including the static pressure coefficient C_{P_s} and the velocity profiles at the inlet of the domain was released by Eckerle [6]. The following steps were taken in order to reproduce this data:

1) The inlet velocity profile given by Eckerle [6] was written into a velocity profile data.

2) A computational domain based on Eckerle's [6] test section was created in Gambit.

3) The mesh of the computational domain created in Step 2, as well as the inlet velocity profile and the boundary conditions used by Eckerle [6] were inserted into Fluent.

4) A pressure based, steady and implicit solver was used. The fully turbulent k-ω model with Shear Stress Transport (SST)

was utilized. A turbulence intensity of 1% and a turbulence length scale of 168 mm (equal to the maximum possible eddy length, which is the cylinder height) were used as the turbulence criteria. A "coupled" pressure-velocity coupling was used for the solution.

The case was then run in Fluent. The static pressure coefficient calculated based on Equation 4, on a cylinder surface line 156 mm above the bottom wall, was used to compare our results and Eckerle's [6]. This line extends from the 0 degree plane to the 90 degree plane.

$$C_{P_S} = \frac{P_{S_{Cylinder}} - P_{S_{Inlet}}}{\frac{1}{2}\rho {U_{Inlet}}^2} \qquad (4)$$

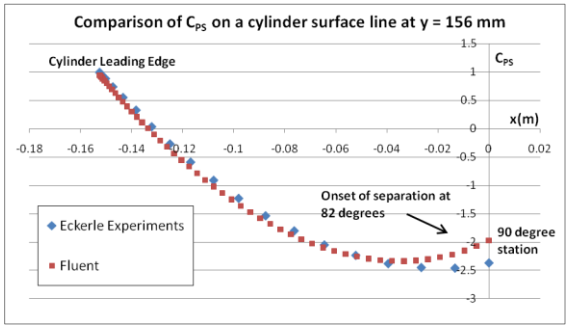

Figure 7. Comparison of C_{P_S} based on a previously published work and on our results

Figure 7 presents a strong proof that the modeling used in Fluent will generate results that show good agreement with experimental results, since the agreement between the two curves is 95% in general.

The second validation study was to conduct a grid independence check before beginning the simulation of each case. Choosing the computational mesh which gives an accurate representation of the flow conditions within the flow domain with the lowest number of three dimensional cells is the aim when looking for grid independence. The most effective way of doing so, is to relate the grid independence to a crucial flow parameter. The static pressure coefficient calculated over a line on the cylinder surface, according to Equation 4, is an example to such a parameter. A grid independence study conducted in this fashion was realized in our previous publications [19], [20] which led to the current paper: The grid independence study indicated that the flow modeling technique used in our studies (the meshing done in Gambit and the flow solution conducted in Fluent) accurately captured the static pressure coefficient, and generated identical results with three different mesh sizes [19], [20]. Hence, a mesh size which will be on the same order of magnitude for all cases was selected for use. The results of the grid independence study and the modeling technique used in our previous work were applied to the current study as well.

Please refer to Gokce [19] and Gokce and Camci [20] for further methodology details, verification methods and geometrical information which are not presented here for the sake of brevity.

RESULTS AND DISCUSSION

Streamline Analysis

Streamlines within the two-dimensional streamwise plane of symmetry and the three-dimensional domain are presented in this section. Note that all plots and videos have been generated using rakes placed at the same exact locations, and with the same exact density for both the baseline and fence-installed cases.

The two-dimensional streamlines originating from the same rakes with the same density are presented in Figures 8 and 9:

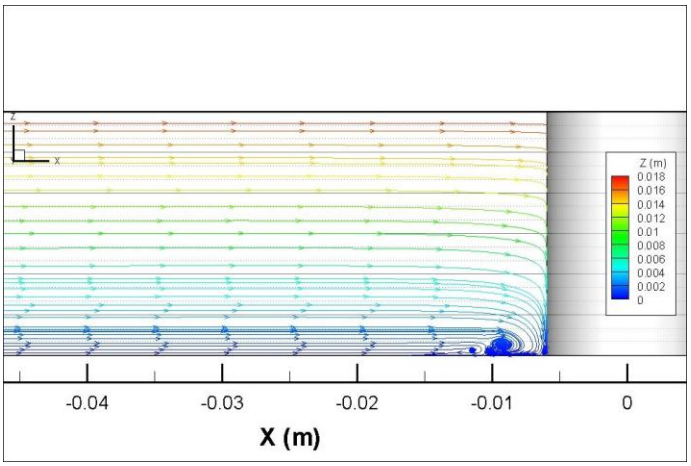

Figure 8. Baseline case: Streamlines within the streamwise plane of symmetry

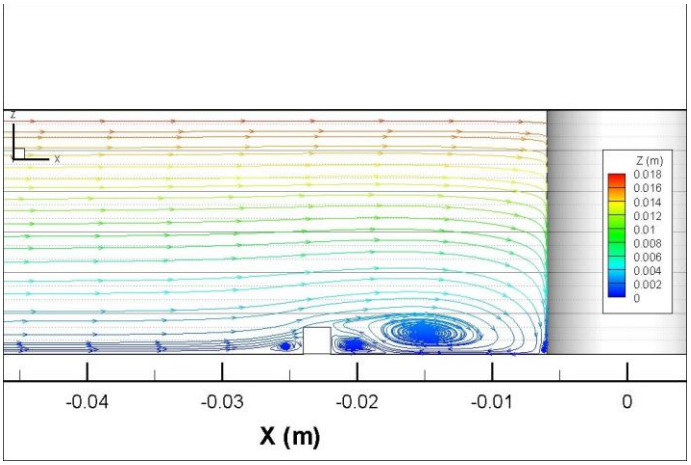

Figure 9. Fence-installed case: Streamlines within the streamwise plane of symmetry

The presence of the fence upstream of the cylinder increases the amount of vortical roll-up within the streamwise plane of symmetry. This situation will lead to increased

turbulent kinetic energy and heat transfer levels, downstream of the cylinder and in the vicinity of the fence-endwall junction.

Video 1:
Upstream 3D Streamlines Baseline
Video 2:
Upstream 3D Streamlines Fence

Videos 1 and 2 demonstrate how the streamlines behave within the domain, upstream of the cylinder. It is observed that, downstream of the cylinder the legs of the horseshoe vortex rise to higher locations within the domain when an upstream fence is employed. This is due to the fact that the main vortex roll-up contains more energy within itself for the fence-installed case, since the increased roll-up brings more high-momentum fluid towards the hub, as observed in Figure 9. In addition, the unsteady vortex shedding is noticed in both cases.

Video 3:
Wake 3D Streamlines Baseline
Video 4:
Wake 3D Streamlines Fence

Videos 3 and 4 demonstrate how the streamlines behave within the cylinder wake. The vortical structure within the wake of the baseline case contains a two-dimensional pattern contained within the x-y plane, whereas the vortical structure within the wake of the fence-installed case contains a more complex three-dimensional pattern.

Total Pressure Contours

The total pressure distribution along x-y planes placed 0.5, 3, 6 and 9 mm above the hub, respectively, are grouped and presented in the following videos for both cases:

Video 5:
Baseline Total Pressure Contours 0.5 mm above hub
Video 6:
Fence Total Pressure Contours 0.5 mm above hub
Video 7:
Baseline Total Pressure Contours 3 mm above hub
Video 8:
Fence Total Pressure Contours 3 mm above hub
Video 9:
Baseline Total Pressure Contours 6 mm above hub
Video 10:
Fence Total Pressure Contours 6 mm above hub
Video 11:
Baseline Total Pressure Contours 9 mm above hub
Video 12:
Fence Total Pressure Contours 9 mm above hub

The comparison of the total pressure contours 0.5 mm above the hub indicate that there is an increase in total pressure levels at the cylinder leading edge-endwall junction for the fence-installed case. However, there is a decrease in total pressure levels, at the location immediately downstream of the fence. This is due to the large impinging and detaching sides of the roll-up: The large impinging side which is close to the cylinder leading edge-endwall junction brings high-momentum fluid towards the endwall and increases the total pressure, whereas the large detaching side takes high-momentum fluid away from the hub and decreases the total pressure near the fence. This observation is also made for the total pressure contours located 3 mm above the hub: The effects of the horseshoe vortex are still seen 3 mm above the hub when an upstream fence is employed. As we proceed from 3 mm to 6 mm and 9 mm above the hub, we note that the effects of the horseshoe vortex are completely gone. Thus, the goal of not affecting the freestream flow after having installed the fence is achieved.

It is noticed that, at 0.5 mm above the hub, the total pressure levels in the cylinder wake is higher for the fence-installed case. This is an indication to a possible local improvement in total pressure. In addition, the unsteady vortex shedding downstream of the cylinder occurs within a larger area: The vortices shed engulf a larger distance along the y-axis. This is due to the generation of a thinner, smaller secondary horseshoe-vortex like structure due to the sharp edges of the fence.

The first of two additional remarks which could be made concerning total pressure is the thin, low total pressure region between the main horseshoe vortex and the secondary horseshoe vortex generated by the fence. Secondly, a more complex shedding mechanism involving a highly turbulent vortical structure is present within the wake of the fence-installed case.

Turbulent Kinetic Energy Contours

The turbulent kinetic energy k distribution along x-y planes placed 0.5, 3, 6 and 9 mm above the hub, respectively, are grouped and presented in the following videos for both cases:

Video 13:
Baseline k Contours 0.5 mm above hub
Video 14:
Fence k Contours 0.5 mm above hub
Video 15:
Baseline k Contours 3 mm above hub
Video 16:
Fence k Contours 3 mm above hub
Video 17:
Baseline k Contours 6 mm above hub
Video 18:
Fence k Contours 6 mm above hub
Video 19:
Baseline k Contours 9 mm above hub
Video 20:
Fence k Contours 9 mm above hub

Similar to the situation existent for the total pressure contours, due to the high momentum fluid it brings towards the

hub, the large impinging side of the main vortical roll-up creates an increase in *k* levels near the cylinder leading edge-endwall junction when a fence is employed, and its large detaching side creates a decrease in *k* levels immediately downstream of the fence.

The *k* contours plotted at each level indicate that the vortex shedding occurs across a larger area downstream of the cylinder when a fence is employed; a point also underlined by the total pressure contours. The complex three-dimensional nature of the wake of the fence-installed case is also visible in the *k* plots drawn at 0.5 mm above the hub.

The turbulent kinetic energy levels within the wake of the cylinder are higher at all heights when a fence is employed; this observation is especially significant within the contours plotted at 0.5 mm above the hub. An increased level of turbulent kinetic energy is an indicator of a possible increase in heat transfer levels.

Heat Transfer Coefficient Contours over the Hub

Videos 21 and 22 depict the heat transfer coefficient contour variations with time for both cases:

Video 21:
Baseline h contours over the hub
Video 22:
Fence h contours over the hub

The structure of the large main vortical roll-up of the fence-installed case imposed its effect on the upstream heat transfer coefficients as well: When compared to the baseline case, a large heat transfer region exists in the vicinity of the cylinder leading edge-endwall junction, while a region of low heat transfer exists just downstream of the fence.

The examination of the wake region of both cases demonstrates a very important result: When an upstream fence is employed, the magnitude of heat transfer coefficient levels downstream of the cylinder is higher. This implies that the usage of an upstream endwall fence will generate increases in heat transfer levels within the cylinder wake: This is a very good result for cooling pin fin applications within the cooling channels of turbine blades.

It should be noted that the runs were calculated with a gas which is hotter than the wall surfaces; the gas side free stream temperature was set to 500 K and the walls to 300 K. This was done in order to model the flow and heat transfer around the NGV blades in a hot gas environment. However, as mentioned before, the model and its heat transfer related results are perfectly applicable to internal cooling system components such as circular pin fins: Even though the walls would be hotter and the heat transfer would be towards the coolant in the case of a circular pin fin, what is important is, the increased magnitude of the heat transfer coefficient levels downstream of the cylinder when an upstream fence is employed.

Spanwise Total Pressure Distribution

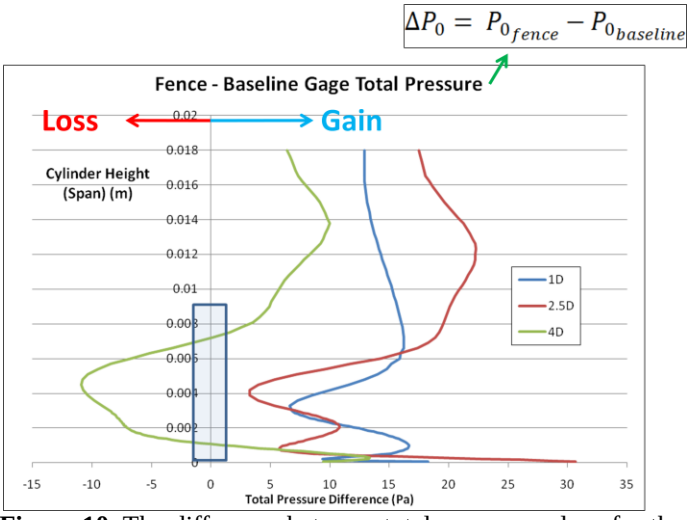

Figure 10. The difference between total pressure values for the two cases, in the spanwise direction

Gage total pressure values are averaged over a series of one dimensional (along the y-axis, domain width) lines having the same streamwise coordinates but varying spanwise (z-direction, along the cylinder height) coordinates. Each z level is assigned an average total pressure value, and the process is repeated for three different locations downstream of the cylinder trailing edge. The difference in these values for the fence-installed and baseline cases, is plotted in Figure 10. The legend denotes the ratio of the streamwise (x-direction) distance between the lines' x-coordinate and the cylinder trailing edge, to the diameter of the cylinder. Note that the results are the average of values taken at 11 time steps, placed 0.4 ms apart. The blue shape in Figure 10 represents the cylinder.

We note that as we move downstream from the cylinder trailing edge, the total pressure levels tend to decrease. We also note that, especially for the 1D and 2.5D locations, the presence of the fence creates an increase in total pressure levels. This situation is beneficial for gas turbine applications, since a higher total pressure level will result in higher efficiency.

Heat Transfer Coefficient Levels

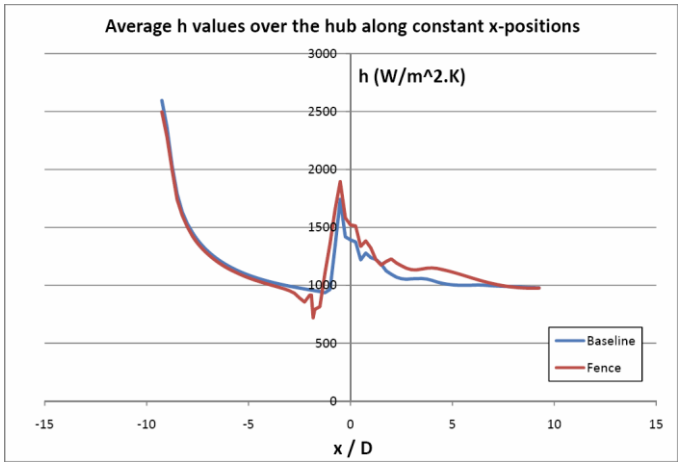

Figure 11. The convective heat transfer coefficient magnitude over the hub along the streamwise axis, plotted for the two cases

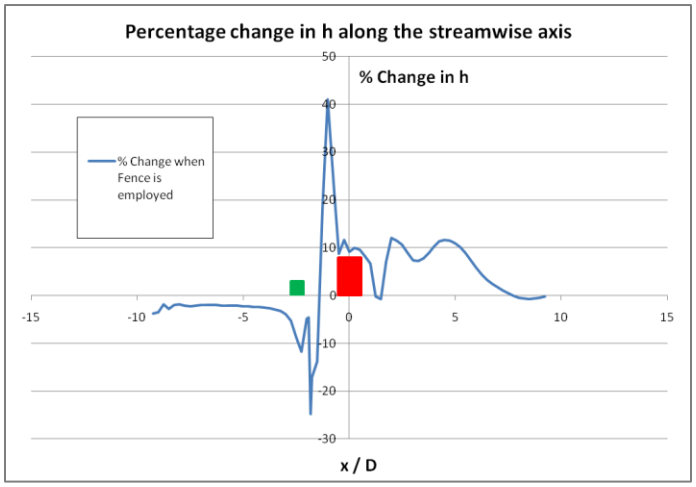

Figure 12. The percentage change in *h* when a fence is employed, when compared to the baseline case

The convective heat transfer coefficient, *h*, is averaged over one-dimensional (in the y-direction, hub width) lines; then, each x/D location is assigned the arithmetic mean of its corresponding line. Figure 11 demonstrates the values for each case, and Figure 12 represents the percentage change in the values when a fence is installed. The green shape shows the location of the fence, and the red shape shows the location of the cylinder.

The results indicate that downstream of the cylinder, the presence of the fence increases the magnitude of the heat transfer rate towards the endwall. The average value of the increase mentioned is around 10% when compared to the baseline case. This situation is beneficial for circular pin fin applications in internal cooling passages, where an increased heat transfer rate will result in more effective cooling.

Mass Averaged Total Pressure Based C_p Analysis

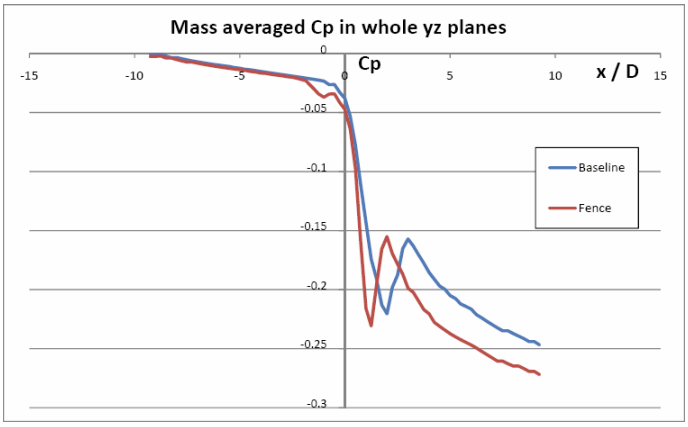

Figure 13. Mass averaged total pressure based C_p values over entire y-z planes

$$C_P = \frac{(P_0)_{YZ\ plane} - (P_0)_{Inlet}}{\frac{1}{2}\rho(U_{Inlet})^2} \qquad (5)$$

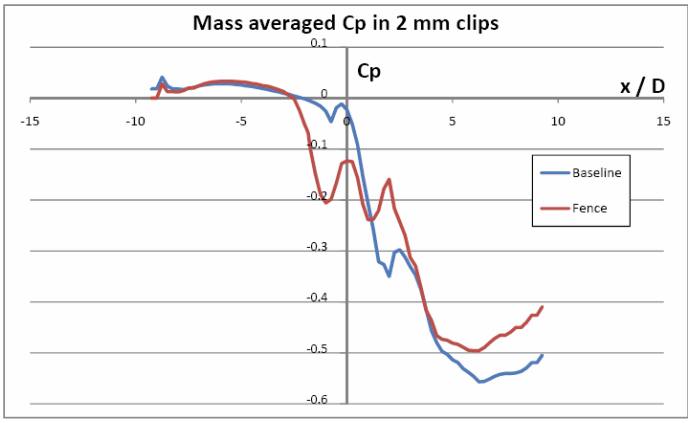

Figure 14. Mass averaged total pressure based C_p values over 2 mm-high rectangular planes extending above the hub surface

$$C_P = \frac{(P_0)_{2\ mm\ Strip} - (P_0)_{2\ mm\ Inlet\ Strip}}{\frac{1}{2}\rho(U_{2\ mm\ Inlet\ Strip})^2} \qquad (6)$$

Figure 13 was plotted using Equation 5, and Figure 14 was plotted using Equation 6.

Figure 13 shows that for the entirety of the domain, the mass averaged total pressure based C_p does not vary greatly when a fence is employed. However, as Figure 14 demonstrates, if the first 2 mm-region above the hub is isolated, it is seen that the presence of the fence creates a noticeable increase in total pressure levels downstream of the cylinder trailing edge. This is a significant feature because any increase in total pressure levels within the turbine is a welcome change. In addition, the immediate vicinity of the fence contains a total pressure drop, as indicated by the large detaching side of the main roll-up.

CONCLUSIONS AND RECOMMENDATIONS

In this paper, the numerical analysis of two flow types, the flow around a NGV and the flow within the cooling channels of turbine blades, is conducted. The NGV blade and the circular pin fin are modeled as vertical circular cylinders in cross flow. The CFD analysis was conducted with the commercially available software Fluent (version 12.1). Many flow properties, including two and three-dimensional streamlines, heat transfer coefficients, total pressure and turbulent kinetic energy contours, are presented.

The main purpose of this study, was to obtain positive results in terms of heat transfer increase and total pressure loss decrease downstream of the cylinder, by placing an endwall fence upstream of a cylinder in cross flow using numerical computations. Therefore, two cases were investigated: First, a baseline case which contains a single vertical circular cylinder placed on an endwall; second, a fence-installed case which contains a 12 mm-wide rectangular fence placed 24 mm upstream of the cylinder center, along with the properties of the baseline case. We also intended to achieve the desired goals without inflicting any modifications to the freestream flow. We have conducted two validation studies in order to assure the accuracy of our CFD modeling strategy: A previously published experimental study's data [6] was re-created and matched using CFD, and a grid independence investigation was also realized.

The comparison of the two cases can be summarized as follows:

1) The presence of the rectangular upstream endwall fence creates a large increase in the size of the main vortical roll-up, located within the streamwise plane of symmetry.
2) The three-dimensional streamline patterns indicate that, when a fence is employed, the legs of the horseshoe vortex rise to higher heights downstream of the cylinder. The cylinder wake of the baseline case contains a two-dimensional vortical structure, whereas the wake of the fence-installed case contains a more complex, three-dimensional vortical structure of higher turbulent nature.
3) Unsteady vortex shedding patterns can be observed for both cases. The unsteady vortex shedding occurs within a larger area when a fence is employed.
4) For the fence-installed case, both the total pressure and turbulent kinetic energy distributions within the cylinder wake, situated very close to the hub, show an increase when compared to the baseline case.
5) Due to the application of the fence, the heat transfer coefficient values downstream of the cylinder increase by an average value of 10%, when compared to the baseline case. This is consistent with the findings of Results 1, 2 and 4.
6) Along the spanwise direction, the presence of the fence creates a gain in the difference between the total pressure values of the fence-installed and baseline cases.
7) Increases in mass averaged total pressure values within the region close to the hub (first 2 mm above the hub) are noticed, when a fence is employed.
8) The freestream was not affected by the presence of the fence.

The rectangular fence installed upstream of the cylinder creates a larger roll-up within the streamwise plane of symmetry, when compared to the baseline case. This roll-up brings high momentum fluid towards the hub, and promotes the increase of total pressure and turbulence levels downstream of the cylinder, when compared to the baseline case. As a result, the increased turbulence levels result in higher heat transfer coefficient values downstream of the cylinder.

The local improvements in total pressure levels near the hub underline an important benefit of using endwall fences in front of NGVs used in gas turbine applications. In addition, the augmented heat transfer values downstream of the cylinder point to the advantage of more effectively cooling turbine blades, when endwall fences are installed upstream of circular pin fins located within blade cooling channels.

The positive results obtained thanks to the placement of upstream endwall fences are encouraging for gas turbine applications. Our research group is currently working on different configurations of the upstream endwall fences and manipulators.

REFERENCES

1. Sieverding, C. H., 1985, *Recent Progress in the Understanding of Basic Aspects of Secondary Flows in Turbine Blade Passages*, ASME Journal of Engineering for Gas Turbines and Power, Vol. 107, pp.248-257
2. Langston, L. S., Nice, M. L., and Hooper, R. M., 1976, *Three-Dimensional Flow Within a Turbine Cascade Passage*, ASME Paper No. 76-GT-50.
3. Mattingly, J. D., *Elements of Propulsion: Gas Turbines and Rockets*, 2nd ed., 2006, American Institute of Aeronautics and Astronautics, Reston, Virginia
4. Hill, P. G. and Peterson, C. R., Mechanics and Thermodynamics of Propulsion, 2nd ed., 1992, Addison-Wesley, Reading, Massachusetts
5. Eckerle, W. A. and Langston, L. S. 1987, *Horseshoe Vortex Formation Around a Cylinder*, ASME Jour. Of Turbomachinery. Vol. 109, pp. 278-285.
6. Eckerle, W.A., *Horseshoe Vortex Formation Around a Cylinder*, Ph.D Thesis, University of Connecticut, Storrs, CT, May 1985
7. Eckerle, W. A. and Awad, J. K. 1991, *Effect of Freestream Velocity on the Three-Dimensional Separated Flow Region in Front of a Cylinder*, ASME Jour. of Fluids Engineering. Vol. 113, pp. 37-44
8. Praisner, T. J. and Smith, C. R. 2006, *The Dynamics of the Horseshoe Vortex and Associated Endwall Heat Transfer-Part I: Temporal Behavior*, Journal of Turbomachinery. Vol. 128, No.4, pp. 747-754
9. Praisner, T. J. and Smith, C. R. 2006, *The Dynamics of the Horseshoe Vortex and Associated Endwall Heat Transfer-Part II: Time Mean Results*, Journal of Turbomachinery. Vol. 128, No.4, pp. 755-762
10. Hada, S., Takeishi, K., Oda, Y., Mori, S., and Nuta,Y. 2008, *The Effect of Leading Edge Diameter on the*

Horse Shoe Vortex and Endwall Heat Transfer, Proceedings of the ASME Turbo Expo, Vol 4, Part A, pp. 813-823

11. Goldstein, R.J. and Karni, J. 1984, *The Effect of a Wall Boundary Layer on Local Mass Transfer From a Cylinder in Crossflow*, Transactions of the ASME. Journal of Heat Transfer. Vol. 106, No. 2, pp. 260-267
12. Camci, C. and Rizzo, D. H., 2002, *Secondary Flow and Forced Convection Heat Transfer Near Endwall Boundary Layer Fences in a 90^o Turning Duct*, International Journal of Heat and Mass Transfer, Vol 45, No. 4, pp. 831-843
13. Rizzo, D. H., *The Aerodynamic and Heat Transfer Effects of an Endwall Boundary Layer Fence in a 90 ^{o} Turning Square Duct*, M.S Thesis, The Pennsylvania State University, State College, PA, May 1994
14. Prümper, H., 1972, *Application of Boundary Fences in Turbomachinery*, AGARD AG No. 164. Paper No. II-3: 315-331
15. VanFossen, G. J., 1982, "*Heat Transfer Coefficients for Staggered Arrays of Short Pin Fins*," ASME J. Eng. Power, 104, pp. 268-284.
16. Metzger, D. E., and Haley, S. W., 1982, "*Heat Transfer Experiments and Flow Visualization for Arrays of Short Pin Fins*," ASME 82-GT-138.
17. Uzol, O. and Camci, C., 2005, "*Heat Transfer, Pressure Loss and Flow Field Measurements Downstream if Staggered Two-Row Circular and Elliptical Pin Fin Arrays*," ASME J. Heat Transfer, 127, pp. 458-471.
18. Chang, S. W., Yang, T. L., Huang, C. C. and Chiang, K. F., 2008, "*Endwall heat transfer and pressure drop in rectangular channels with attached and detached circular pin-fin array*," International Journal of Heat and Mass Transfer, 51, pp. 5247-5259
19. Gokce, Z. O. *Comparative Numerical Analysis of Flow Development in the Presence of Endwall Fences Upstream of a Vertical Cylinder in Cross Flow*. M.S Thesis, The Pennsylvania State University, PA, May 2010.
20. Gokce, Z. O. and Camci, C., 2011, *Aerodynamic Influence of Endwall Fences Located in the Vicinity of the Leading-Edge Endwall Junction of Nozzle Guide Vanes*, ASME 2011 International Mechanical Engineering Congress and Exposition, ASME/IMECE2011-65255, November 11-17 2011, Denver, Colorado, In Publication
21. Turgut, H. O., 2007-Present, Private Communications, The Pennsylvania State University
22. Kavurmacioglu, L., Dey, D. and Camci, C. July 2007, *Aerodynamic Character of Partial Squealer Tip Arrangements in an Axial Flow Turbine, Part I: Detailed Aerodynamic Field Modifications via Three Dimensional Viscous Flow Simulations Around Baseline Tip*, Progress in Computational Fluid Dynamics, Vol. 7, pp. 363-373
23. Kavurmacioglu, L., Dey, D. and Camci, C. July 2007, *Aerodynamic Character of Partial Squealer Tip Arrangements in an Axial Flow Turbine, Part II: Detailed Numerical Aerodynamic Field Visualizations via Three Dimensional Viscous Flow Simulations Around a Partial Squealer Tip*, Progress in Computational Fluid Dynamics, Vol. 7, pp. 374-386
24. Rao, N., Kavurmacioglu, L., Gumusel, B. and Camci, C., 2006, *Influence of Casing Roughness on the Aerodynamic Structure of Tip Vortices in an Axial Flow Turbine*, ASME Paper GT2006-91011, presented at the ASME International Gas Turbine Congress in Barcelona, Spain.
25. Zaccaria, M. A., *An Experimental Investigation into the Steady and Unsteady Flow Field in an Axial Flow Turbine*, Ph.D Thesis, The Pennsylvania State University, State College, PA, December 1994.